

# High Efficiency and High Rate Deposited Amorphous Silicon-Based Solar Cells

PHASE III Fourth Quarter  
Technical Progress Report

June 1, 2004 to August 31, 2004

**NREL Subcontract No. NDJ-2-30630-08**

Subcontractor: The University of Toledo

Principal Investigator: Xunming Deng  
Department of Physics and Astronomy  
University of Toledo, Toledo, OH 43606  
(419) 530-4782  
dengx@physics.utoledo.edu

Contract technical monitor: Dr. Bolko von Roedern

# Amorphous Silicon Based Minimodules with Silicone Elastomer Encapsulation

Contributors: Aarohi Vijh and Xunming Deng

## Introduction

Ethyl vinyl acetate (EVA) is the most commonly used material for the encapsulation of terrestrial solar cells. It is well known that EVA turns yellow upon extended exposure to ultraviolet light. This yellowing upon exposure to UV light is a characteristic of most carbon based polymers. Silicon-based polymers (silicones) may not show this effect. Although silicones were used to encapsulate solar cells in the 1970s and 1980s, they were dropped in favour of ethyl vinyl acetate due to its lower cost [1]. However, the price of silicone elastomers has come down over the years and their quality and ease of application have improved, which may make them suitable for encapsulating solar cells once again. We have recently fabricated 4"x 4" and 4"x8" minimodules encapsulated with a combination of a silicone elastomer and Dupont Tefzel.

## Experimental Details

The silicone used in our experiments was Dow Corning's Sylgard 182. Sylgard 182 is a blend of silanes ( $-\text{Si}-$ )<sub>n</sub> and siloxanes ( $-\text{Si}-\text{O}-\text{Si}-$ )<sub>n</sub> with alkyl groups substituting some of the hydrogen atoms, i.e. it has a silicon backbone, which makes it different from carbon based polymers such as EVA. Glass slides were encapsulated on both sides with EVA/Tefzel and silicone elastomer/Tefzel in a vacuum laminator. The EVA was obtained from Specialized Technology Resources. Figure 1 compares the light transmission of these samples with that of a plain glass slide.

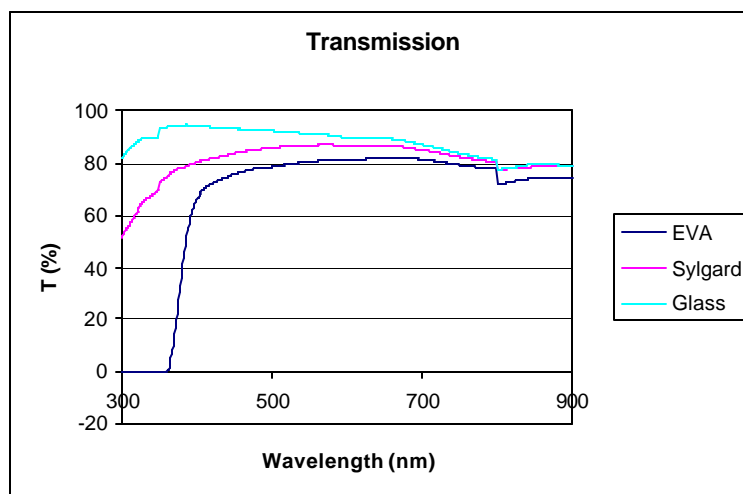


Figure 1: Transmission of glass encapsulated with EVA and Sylgard.

In the thickness applied, the Sylgard-encapsulated slide showed better light transmission throughout the visible wavelength range than the EVA encapsulated slide. Its UV cutoff was more gradual than that of EVA, which blocked all light of wavelength shorter than 360 nm.

Two minimodules were then fabricated from 4"x4" single junction amorphous silicon-germanium solar cells and encapsulated with Sylgard 182 and Tefzel in the vacuum laminator. The first minimodule had a single 4"x4" a-SiGe n-i-p cell while the second consisted of two 4"x4" cells in series. Each cell had an active area of approximately 81 cm<sup>2</sup>. Current collection grids consisting of tinned copper wire applied to the ITO front contact with conductive silver paint for the series interconnected cells, and conducting graphite paint for the single cell. Reverse-protection diodes were also attached between the bus bars of the cells. Before application of grids, the cells were shunt-passivated using a light-assisted electrochemical method [2], details of which will be reported separately. The cells were then vacuum laminated with Sylgard 182 and Tefzel at 125°C for 30 minutes. Being a liquid, Sylgard 182 flows well, and no trapped bubbles were found in the laminated minimodules. Coverage of raised features (e.g. the diodes and grid lines) was excellent. Figure 2 shows a photo of the 4"x4" and 4"x8" minimodules. The discolouration on the surface of the cells is a result of the shunt passivation process.

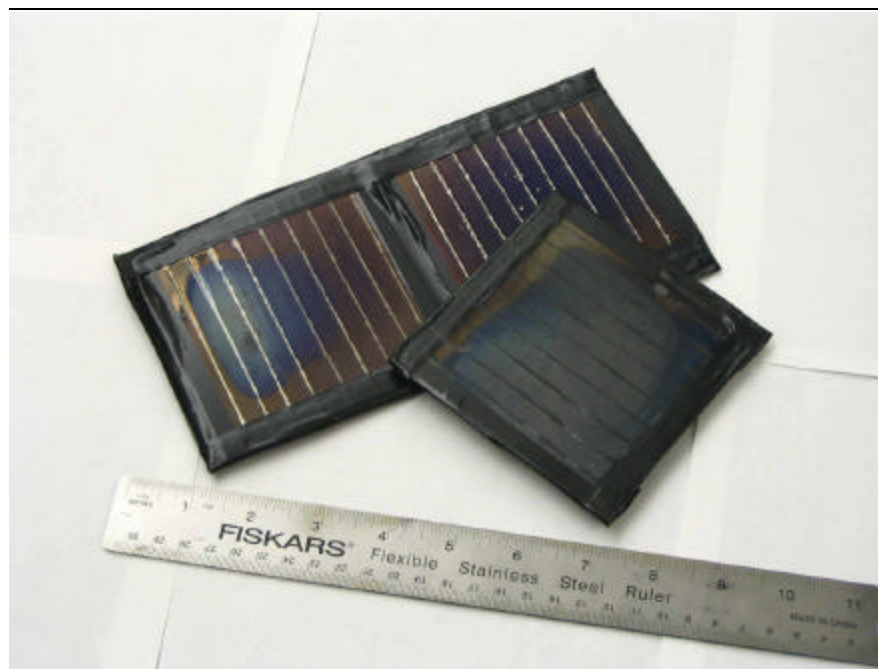


Figure 2: Silicone elastomer encapsulated a-SiGe based minimodules

The cells produced the expected open circuit voltages of 0.8 V and 1.6 V for the single and two-cell minimodules, respectively. The short circuit current was 183 mA for the 4"x4" minimodule, and 760 mA for the 4"x8" interconnected minimodule, corresponding to current densities of 2.2 and 9.4 mA/cm<sup>2</sup>, respectively. The currents were limited by the series resistance of the grids and interconnects, which at approximately 1  $\Omega$  per cell for the silver

paint-attached grids and 4  $\Omega$  per cell for the carbon paint-attached grids, were excessive for the expected  $I_{sc}$  of  $\sim 1.6A$ . With the reverse protection diodes removed and under a reverse bias, the current in the 4"x8" minimodule increased to approximately 1.0A.

## Conclusion

Both minimodules encapsulated with silicone elastomer functioned well. The quality of the encapsulant in terms of adhesion and bubble-free lamination was found to be good. Its light transmission for the thickness applied was found to be better than that of EVA. We conclude that silicone elastomers can be used as an alternative encapsulant for encapsulating solar cells.

## References

- [1] Muirhead, I.J. and Hawkins, B.K., *An assessment of photovoltaic power in the Telstra network*, Annual Conference of the Australian and New Zealand Solar Energy Society – SOLAR, 1995
- [2] Vijn, A. and Deng, X., *Light Assisted Shunt Passivation for Amorphous Silicon Photovoltaics*, Patent Application submitted to USPTO, April 2004.

# Measurement of Component-Cell Current-Voltage Characteristics in a Tandem-Junction Two-Terminal Solar Cell

Contributors: Chandan Das, Xianbi Xiang and Xunming Deng

## Abstract

A new method for measuring component cell current-voltage (I-V) characteristics in a tandem-junction two-terminal solar cell is described. The measurements are performed with (a-Si/a-SiGe) tandem structure solar cell using two separate light beams of different wavelengths. The I-V characteristics of the component cells are obtained and open-circuit voltage ( $V_{oc}$ ), short-circuit current ( $I_{sc}$ ) and fill-factor (FF) are calculated. This method could be a useful tool for evaluation and optimization of multijunction solar cells.

## Introduction

In the course of fabricating and optimizing multiple-junction, two-terminal solar cells, it is important to be able to determine the performance of the individual component cells, since a separate single cell, even fabricated under the same conditions, may perform differently from the corresponding component cell within a multiple junction stack. Some differences are reproducible, such as those due to differences in the sub-structure; however, other differences can arise from unrecognized or uncontrolled parameters. The latter is particularly true for production processes insofar as all cells fabricated under identical conditions should have identical performance, but from time to time, are different due to unrecognized parameter variations. Sometimes there are even unidentified catastrophic changes. Without a technique to measure component cell performance in the multiple-junction stack, one could not identify immediately which of the component cells failed or degraded and, therefore, important production time for a multijunction device manufacturer would be wasted. Kurtz et. al. [1] developed a process to measure component cells in a tandem device. However, these approaches call for an initial estimate of the component cell  $V_{oc}$ . If the initial estimate is not accurate, different results may be obtained. Thus, the applicability of this method is limited. In this work, we report the use of a new technique developed at the University of Toledo [2] to measure component cell I-V in a tandem stack without any initial assumptions.

## Outline of Methodology

In order to extract the information about current of a component cell in a tandem stack, where the components cells rely on spectrum-splitting absorption, one could easily make the tandem current limited by one component, by flooding the other component with a proper color of light. Thus under such a condition, the current of the one component could be measured and I-V could be drawn. However, to get information about individual voltage of each component, there is no such direct way and in a two terminal device structure, voltage is always measured as the sum of the two component voltage. Therefore, the challenge is that,

to get the information about the contribution of voltage from each component in the total tandem voltage. The following procedure deals with this problem.

The procedures for measuring component-cell I-V characteristics consist of two major parts: 1) measurement of open circuit voltage ( $V_{oc}$ ) of each of the component cells inside a tandem cell; and 2) measurement of the short circuit current ( $I_{sc}$ ) and fill factor (FF) of the component cells.

To illustrate the measurement procedures, we will describe in detail the measurement of top component cell in a two-terminal, tandem-junction a-Si/a-SiGe solar cell.

Step 1: Measurement of  $V_{oc}$  of each of the component cells under a given illumination

This step consists of several sub-steps:

- 1A) Measure the relationship between  $V_{oc}$  (top) and  $I_{sc}$  (top) for the top component cell;
- 1B) Measure the relation between  $V_{oc}$  (bottom) and  $I_{sc}$  (bottom) for the bottom component cell;
- 1C) Measure  $I_{sc}$  (top) and  $I_{sc}$  (bottom) under a given illumination;
- 1D) Obtain the  $V'_{oc}$  (top) and  $V'_{oc}$  (bottom) from the calibration curves generated in Steps 1A and 1B for the top and bottom cells under the given illumination corresponding to the  $I_{sc}$  values obtained in Step 1C; and
- 1E) Compare [ $V'_{oc}$  (top) +  $V'_{oc}$  (bottom)] with the measured  $V_{oc}$  (tandem) to obtain  $V_{oc}$  (top) and  $V_{oc}$  (bottom) under this given illumination.

Step 2: Measurement of  $I_{sc}$  and FF of component cells

- 2A) Put the tandem cell under top-cell current limiting condition, i.e., stronger red illumination and relatively weaker blue illumination and scan the I-V of the tandem cell.
- 2B) Subtract the voltage of the tandem cell with  $V_{oc}$  of the bottom cell, obtained above, for this given illumination. Replot the I-V curve of the tandem cell after  $V_{oc}$ (bottom) is subtracted under the illumination in which the tandem-cell current is limited by that of the top cell. This replotted curve is the I-V characteristics of the top component cell.
- 2C) Put the tandem cell under bottom-cell current limiting condition and repeat the these steps to obtain the bottom cell I-V characteristics.

## Description of the Procedures and Results

Step 1: Measurement of  $V_{oc}$  of each of the component cells under a given illumination

Step 1A: First, to make sure that the relationship between  $V_{oc}$  and  $I_{sc}$  of an a-Si or a-SiGe cell is independent or weakly dependent at most, on the wavelength of the illumination, single-junction a-Si and a-SiGe cells are used and measured under various monochromatic lights. It is found that the  $V_{oc}$  vs  $I_{sc}$  curves are indeed independent of the wavelength of the illumination as shown in Fig. 1 and Fig. 2 for top and bottom single junction cells respectively. In the discussions afterward, all measurements are carried out in a two-terminal

tandem structure. The quantum efficiency of the a-Si/a-SiGe tandem cell is measured using a method developed by Burdick and Glatfelter [3].

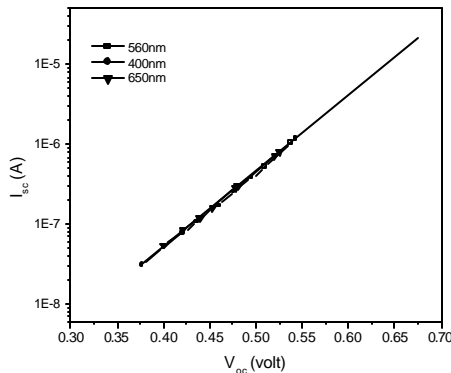


Fig. 1 Relation between  $I_{sc}$  and  $V_{oc}$  of single junction top cell under different wavelength of monochromatic light

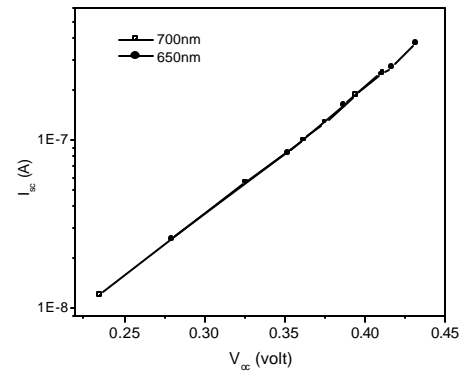


Fig. 2 Relation between  $I_{sc}$  and  $V_{oc}$  of single junction bottom cell under different wavelength of monochromatic light

The tandem cell is illuminated with a blue light; a 400 nm monochromatic light is used in this measurement so that the blue light is fully absorbed by the top cell and the bottom cell is in dark. Fig. 3 shows that the bottom-cell QE at 400nm is zero. Under the 400 nm blue light, the bottom cell is in dark and does not contribute to the tandem cell  $V_{oc}$ . Extreme care was made to make sure that there is no scattered red light near the sample. The  $V_{oc}$  of the tandem cell, therefore, is approximately the  $V_{oc}$  of the top cell,  $V_{oc}$  (top), under this 400 nm light. The current of the tandem cell is, however, limited by the current of the bottom cell. To measure the current of the top cell, a relatively more intense red bias light, obtained from a tungsten lamp with a 610 nm long-pass filter, is illuminated on the tandem cell so that the current of tandem cell is limited by the top cell. By taking the difference of the tandem-cell  $I_{sc}$  with and without the 400 nm blue light, the  $I_{sc}$  of the top cell,  $I_{sc}$  (top), under this particular 400 nm light is obtained. Varying the intensity of the 400 nm blue light, the relationship of  $V_{oc}$  (top) and  $I_{sc}$  (top) is obtained, as shown in Fig. 4. It is possible that the  $V_{oc}$  (top) vs  $I_{sc}$  (top) relationship shown in Fig. 2 is slightly different from the actual relationship since there might be small contribution of the voltage from the bottom cell under 400 nm light.

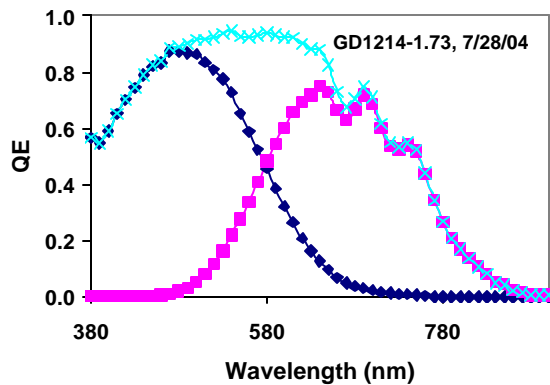


Fig. 3 Quantum efficiency curves of a tandem-junction a-Si/a-SiGe solar cell used in this study to illustrate the method.

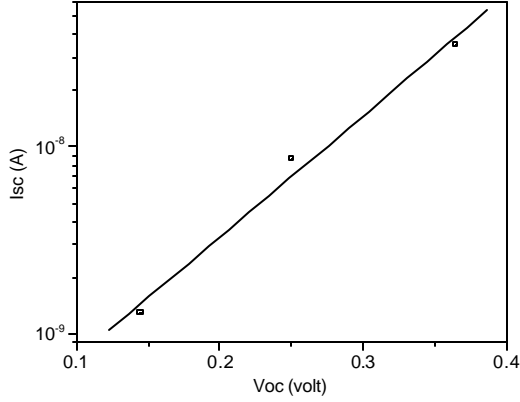


Fig. 4:  $I_{sc}$  vs  $V_{oc}$  plot with varying intensity of 400 nm light intensity for top component cell.

Step 1B: a similar approach is taken for measuring the  $V_{oc}$  (bottom) and  $I_{sc}$  (bottom) relationship except that in this case the red light is a 700 nm monochromatic light and the blue light is from the tungsten lamp with a 470 nm short-pass filter. Under the 700 nm red light, the top cell is in dark and does not contribute to the tandem cell  $V_{oc}$ . The tandem cell  $V_{oc}$  is therefore the  $V_{oc}$  of the bottom cell. The blue bias light allows one to measure  $I_{sc}$  (bottom). The obtained  $V_{oc}$  (bottom) and  $I_{sc}$  (bottom) relationship is shown in Fig. 5.

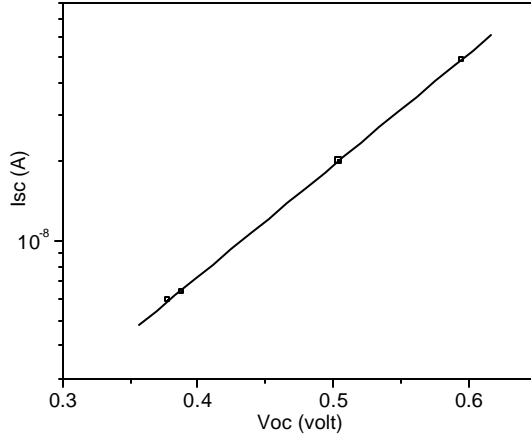


Fig. 5:  $I_{sc}$  vs  $V_{oc}$  plot under varying intensity of 700 nm light for bottom component cell.

Step 1C: Under a given illumination, the  $I_{sc}$  (tandem) is either  $I_{sc}$  (top) or  $I_{sc}$  (bottom) depending on the relative intensity of the blue and red light. Fig. 4 shows the  $I_{sc}$  of a tandem cell under illumination of a fixed-intensity blue light and a varying-intensity red light. The  $I_{sc}$  (tandem) is plotted against the intensity of the red light measured with a detector voltage response. At the highest red-light intensity, the current of the tandem cell is limited by the top-cell current and with the decrease of the red-light intensity to a certain level, this current remains almost constant. Further reduction of red-light intensity makes the tandem cell current to be limited by the bottom-cell current and thus the tandem-cell current decreases with the red-light intensity. The point of inversion, where the dependence on limitation of component current shifts, is obtained by the sharp change of the slope of the curve. At this point, both the component cells have same current, i.e.  $I_{sc}(\text{top}) = I_{sc}(\text{bottom}) = 4.54 \times 10^{-8}$  A, for the sample shown in Fig. 6. Generally, at low red-light intensity, the tandem-cell current is limited by the bottom cell, while at high red-light intensity, the tandem is limited by the top



cell. By increasing the red and blue light separately from a given illumination, one can determine the  $I_{sc}$  (top) and  $I_{sc}$  (bottom) of the tandem cell under this given illumination.

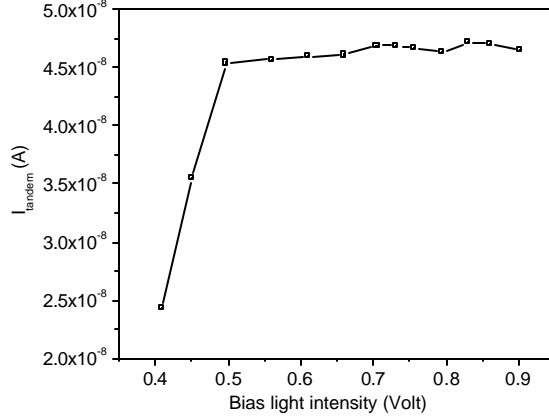


Fig. 6: Tandem cell current under varying intensity of red bias light.

Step 1D: The  $V_{oc}$  of the top and bottom component cells of the tandem cell under the given illumination is then obtained from the  $I_{sc}$  (top) and  $I_{sc}$  (bottom) values from Step 1C and the  $I_{sc}$  vs  $V_{oc}$  relationships from Steps 1A (Fig. 4) and 1B (Fig. 5). A given illumination is used as an example to illustrate the procedures. Under this illumination, the  $I_{sc}(\text{top})$  and  $I_{sc}(\text{bottom})$  as determined from Step 1C were  $3.7 \times 10^{-8} \text{ A}$  and  $4.54 \times 10^{-8} \text{ A}$ , respectively. The  $V_{oc}$  (tandem) under this given illumination is measured to be 0.815V. Using the  $I_{sc}$  vs  $V_{oc}$  curves established in Step 1A (Fig. 4) and Step 1B (Fig.5), the calculated open circuit voltages for the top and bottom cells,  $V'_{oc}(\text{top})$  and  $V'_{oc}(\text{bottom})$ , are 0.354V and 0.593V, respectively, and the total combined voltage,  $V'_{oc}(\text{tandem})$ , is 0.947V.

Step 1E:  $V'_{oc}(\text{tandem})$  is higher than 0.815V, the measured value for  $V_{oc}(\text{tandem})$ . This is because during Step 1A (Step 1B) when the tandem cell is illuminated with blue (red) light, the bottom (top) cell may generate a small voltage even though most of the blue (red) light is absorbed by the top (bottom) cell. Assuming that the error introduced in Steps 1A and 1B are about the same magnitude, we obtained the  $V_{oc}(\text{top}) = V'_{oc}(\text{top}) \times [V_{oc}(\text{tandem}) / V'_{oc}(\text{tandem})] = 0.305 \text{ V}$  and  $V_{oc}(\text{bottom}) = V'_{oc}(\text{bottom}) \times [V_{oc}(\text{tandem}) / V'_{oc}(\text{tandem})] = 0.510 \text{ V}$ , under the given illumination in this example.

## Step2. Measurement of $I_{sc}$ and FF of component cells

Step 2A: The tandem cell is put under the illumination described above, which generates higher  $I_{sc}$  (bottom) than  $I_{sc}$  (top). A varying electrical bias is applied on the tandem cell to scan the  $I(\text{tandem})$  vs  $V(\text{tandem})$  characteristics. In this case,  $I(\text{tandem})$  is  $I(\text{top})$  since the current of the tandem cell is limited by that of the top cell.

Step 2B: Near the maximum-power operating point of the tandem device in which the current is limited by the top, the voltage of the bottom cell is approximately  $V_{oc}$  (bottom). Subtracting  $V_{oc}$  (bottom) obtained in Step 1E, we obtain the voltage of the top cell  $V(\text{top}) = [V(\text{tandem}) - V_{oc}(\text{bottom})]$ , which, combined with the  $I(\text{top})$ , provides the I-V characteristics of the top component cell, as shown in Fig. 7 for the given illumination described above.

Step 2C: A different illumination which has stronger blue light, is used to measure the component cell I-V characteristics of the bottom cell. The result is shown in Fig. 8.

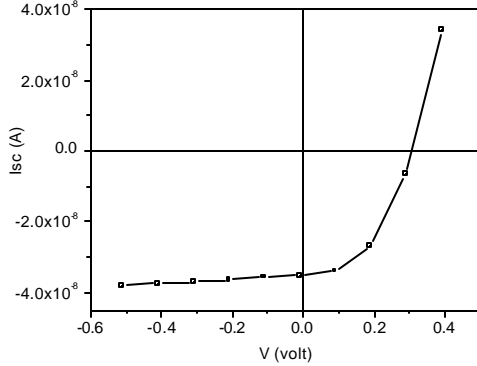


Fig. 7: I-V characteristic of top component cell.

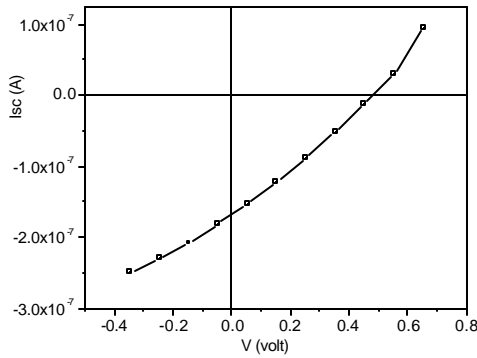


Fig. 8: I-V characteristic of bottom component cell.

The I-V curves shown in Figures 7 & 8 represent the I-V curves of the top and bottom component cells in the a-Si/a-SiGe tandem-junction solar cell under the given illumination. The FF for the top and bottom components under this illumination are calculated as 0.48 and 0.27 respectively. Same method could be used to determine the I-V characteristic for the device under 1-sun illumination.

## Conclusion

A new method to measure the component cell I-V characteristics of a multiple-junction, two-terminal cell has been developed [2] and described. The new method is demonstrated to measure the component-cell I-V characteristics of the tandem-junction cell effectively. Further works are ongoing to demonstrate the method for 1-sun illumination and for triple-junction solar cells.

## Reference:

- [1] S. Kurtz, K. Emery and J. M. Olson, Proc. of 1<sup>st</sup> WCPEC, 1773 (1994).
- [2] X. Deng, "Method for Measuring Component Cell Current-Voltage Characteristics in a Multi-junction, Two-terminal Stacked Solar Cell", University of Toledo Invention Disclosures for Patent Application, April 11, 2002 and July 9, 2004.
- [3] J. Burdick and T. Gletfelter, 18, 301 (1986).